Ethylene-Octene Copolymer-Nanosilica Nanocomposites: Effects of Epoxy Resin Functionalized Nanosilica on Morphology, Mechanical, Dynamic Mechanical and Thermal Properties

Chaganti Srinivasa Reddy,[*1] *Prabir Kumar Patra,*[2] *Chapal Kumar Das*[1]

Summary: A comparative study of the structural, thermal, mechanical and thermo-mechanical properties of ethylene-octene copolymer[1] (*mPE*)[2] nanocomposites synthesized with *pure nanosilica* (*NS*) and nanosilica-functionalized with *diglycidyl ether of bisphenol-A* (*ENS*) has been reported. These nanocomposites were prepared using ''melt mixing'' method at a constant loading level of 2.5 wt. %. The effects of pure nanosilica (*NS*) and epoxy resin-functionalized-nanosilica (*ENS*) on the above mentioned properties of ethylene-octene copolymer were analyzed by wide-angle-x-ray diffractometer (WAXD), transmission electron microscope (TEM), thermo gravimetric analyzer (TGA), differential scanning calorimeter (DSC), dynamic mechanical analyzer (DMA) and scanning electron microscope (SEM). TEM studies have shown a better dispersion of nanoparticles in case of ethylene-octene copolymer-epoxy resin-functionalized-nanosilica nanocomposite (*mPE-ENS*) than that of ethylene-octene copolymer-nanosilica nanocomposite (*mPE-NS*). The tensile tests show that organic modification of nanosilica particles brings up an appreciable increase in yield strength, ultimate tensile strength and elongation at break of the polymer. DMA studies have shown an increase in the storage modulus and glass transition temperature for *mPE-ENS* with respect to *mPE-NS*. Further, the TGA results have shown a higher thermal stability for *mPE-ENS* in comparison to *mPE-NS*.

Keywords: epoxy resin; functionalization; interfaces; nanoparticles; mechanical properties and thermal properties; nanocomposites

Introduction

In recent years, the development of Dow's INSITE™ constrained geometry catalyst technology has led to the development of a new class of elastomers based on homogeneous ethylene-α-olefin copolymers. In general, ethylene-octene copolymers with more than 8 wt. % octene content form a unique class of elastomers. These copolymers possess low crystallinity and rubber-like behavior that depends on physical junctions.[1] The main advantage of these copolymers over chemically vulcanized elastomers lies in their ease of processing and post-processing, much like conventional polyethylene. These elastomeric materials have been commercialized and are the subject of numerous investigations

[1] Materials Science Centre, Indian Institute of Technology, Kharagpur-721302, India
E-mail: mecsreddy@yahoo.com; ckd@matsc.iitkgp.ernet.in
[2] Department of Materials and Textiles, University of Massachusetts Dartmouth 285 Old Westport Road, North Dartmouth, MA 02747, USA

[1]Ethylene-octene copolymer is produced using Dow's ***INSITE***™ constrained geometry catalyst and process technology. ***ENGAGE*** the trade name of this copolymer.
[2]This copolymer will be represented as ***mPE***.

as unfilled and filled polymers.[2–4] Especially, commercially available copolymers with more than 25 wt. % octene are an extremely important class of elastomers because of their high filler loading capacity. The backbone of these elastomers is a saturated carbon skeleton that can be efficiently cross-linked by peroxide, irradiation or a silane-coupling agent.

Silica is being used extensively in different rubbers as reinforcing filler for many years. Recently, nanosilica, owing to its large specific surface area, has become very popular for synthesizing polymer nanocomposites. The research on nanosilica-based composites is mainly focused on improving the mechanical and optical properties of polyolefins. Ray et al.[5] were studied the influence of untreated silica and electron-beam-modified-surface coated silica filler on the dynamic mechanical and thermal properties of ethylene-octene copolymers.

Now, the preparation of a composite material by melt-blending a polymer and filler is a straightforward procedure. But due to the agglomeration of nanoparticles it is less efficient when the reinforcing filler is in nanoscale dimension. To overcome this limitation, a first strategy[6] had been proposed earlier. It explains a technique based on encapsulation of the filler by a polymer coating. A second approach[7] was also proposed which relies upon the chemical modification of the filler surface by functional silanes and titanate esters. The titanate esters and functional silanes actually promote adhesion of the filler to the polymer matrix.[7–12] A worldwide total of about 16,000 tons of coupling agents worth around US$180 million is consumed annually for chemical functionalization of around 1.5 million tons of fillers. However, the high cost of functional silanes limits their production and applicability.

In the earlier work of authors[13] it was shown that low-density polyethylene filled with *ENS* provides an improvement in mechanical properties and thermal stability of the low-density polyethylene matrix at a much lower loading level of 2.5 wt. %. It was also shown that this improvement was even more than when nanosilica was modified with a silane-coupling agent.

The main objective of the present investigation is to evaluate the enhanced influence of epoxy resin functionalized nanosilica filler over pure nanosilica on the properties of ethylene-octene copolymer (*ENGAGE*) when present in similar concentration of 2.5 wt%. To support this study various results showing improvements in the structural, thermal, mechanical and dynamic mechanical properties of ethylene-octene copolymer and synthesized nanocomposites have been included.

Another noticeable point is that ''*melt blending*'' technique had been used to prepare the composite samples because it is an industrially viable method for mass production

Experimental Part

Materials

Ethylene-octene copolymer[3] (*ENGAGE-8440, represented as mPE*[4]) containing 2.3-wt % octene was kindly provided by DuPont-Dow Elastomers, USA. *Nanosilica* (*NS*) was obtained from the Department of Chemistry, IIT Kharagpur, India; and the particles were synthesized using sol-gel method. The particle size of the *nanosilica* was in the range of 25 *nm* -35 *nm* and the specific surface area was 360 m^2/g. The particles were spherical and amorphous. The epoxy resin was a liquid *diglycidyl ether of bisphenol-A* (*DGEBA*) (*Ciba Geigy, Araldite LY 556*) with an equivalent weight per epoxide group of 195 ± 5 – *used as received*. *Tin* (*II*) *chloride* and *methyl isobutyl ketone* (*MIBK*) were obtained from MERCK India limited – *used as received*. The International Union of Pure and Applied Chemistry (IUPAC) recommended names of the polymer was not used, where as the source name of the polymer was used.

[3]Ethylene-octene copolymer is produced using Dow's ***INSITE***™ constrained geometry catalyst and process technology. ***ENGAGE*** is the trade name of this copolymer.

[4]This copolymer is represented as ***mPE***.

Surface Functionalization of Nanosilica with Epoxy Resin

The reaction of silica particles with epoxy resin (*DGEBA*), an organic functionalizing agent, was carried out as follows. Nanosilica (*NS*) particles were suspended in methyl isobutyl ketone solvent. Epoxy resin was then added to the resulting solution. The weight ratio of nanosilica and epoxy resin was taken as 40:60. After adding 1000 ppm of $SnCl_2$ as catalyst to this suspension, it was introduced into a three-necked- round-bottomed flask equipped with a mechanical stirrer, a water condenser and a thermometer. The reaction was carried out at 140 °C for 2 h. The solvent was then removed with a rotary evaporator and the product was dried in vacuum oven for 1 h. The dried sample was then used for spectroscopy analysis. Fourier transform infrared spectroscopy experiments were done on *NS* and *ENS* using a NEXUS 870 FTIR (Thermo Nicolet) in humidity less atmosphere and at room temperature.

Preparation of Nanocomposites

Nanocomposites were prepared using "*melt blending*" method in a sigma- internal-mixer. In the first mix, *mPE* was melt mixed with *NS* at 150 °C for 10 min at a fixed internal rotor speed of 100 r.p.m. In the second mix *mPE* was melt mixed with *ENS* using the same procedure and conditions. The formulations for the composites are given in Table 1. The composites thus obtained were hot pressed using compression mold at 150 °C for 10 min. and at a constant pressure of 10 MPa. Composite sheets thus obtained were allowed to cool down to room temperature at a rate of 2 °C/min under the applied pressure to allow slow crystallization of the samples.

Methods and Measurements

Transmission Electron Microscopy (TEM)

TEM samples were ultramicrotomed with a diamond knife on a Leica Ultracut UCT microtome at room temperature to give sections with a nominal thickness of 50 nm. The sections were transferred from water to carbon-coated Cu grids of 200 mesh (0.127 mm). High-resolution TEM images of *mPE* nanocomposites were obtained at an operating voltage of 200 kV, with the sample working pressure (vacuum) of 10–5 Pa, under low-dose conditions, with a JEOL JEM-2100 TEM, equipped with a LaB_4 electron gun. Imaging was conducted using a Gatan slow scan CCD camera with 1024×1024 pixel resolution. The contrast between the nanofillers and the polymer phase was sufficient for imaging, so no heavy metal staining of sections prior to imaging was required.

Mechanical Property Studies

The dumb-bell shaped testing samples were cut from the molded sheets and were used for tensile testing at least 24 h after molding. Tensile test was carried out using the *Hounsfield HS 10 KS* (*universal testing machine*), at room temperature with an extension speed of 5 mm/min and an initial gaze length of 35 mm. The results reported are the averages of four samples for each composite; each result with an experimental error of ±2%.

Dynamic Mechanical Analysis

Dynamic mechanical analysis (DMA) was carried out using TA instruments' *DMA-2980*–Dynamic Mechanical analyzer. The instrument was used in the single-cantilever-bending mode. The samples were subjected to a sinusoidal displacement of

Table 1.
Compounding formulation of mPE nanocomposites.

Sample configuration	Composition (wt %)		
	mPE	Nanosilica (NS)	Epoxy resin-functionalized-nanosilica (ENS)
mPE	100	0	0
mPE-NS	100	2.5	0
mPE-ENS	100	0	2.5

0.1% strain at a fixed frequency of 1 Hz from −100 °C to +100 °C with a heating rate of 10 °C/min. The *storage modulus* (*E'*) and *loss tangent* (*tan δ*) were measured for each sample in this temperature range.

Thermogravimetric (TG) and Differential Scanning Calorimetric (DSC) Studies

Thermal stabilities of the composites were studied using the *TGA V 50 1A DuPont 2100* thermogravimetric analyzer in presence of air from 50 to 700 °C, at a heating rate of 10 °C/min. Differential scanning calorimetric study was carried out in an inert atmosphere of nitrogen with the *TA DSC Q1000 V7.0 – Differential Scanning Calorimeter*. The data has been reported for the second heating and second cooling run from 60 °C to 200 °C at 10 °C/min.

Scanning Electron Microscopy (SEM)

Scanning Electron Microscopic analysis was done using the *JEOL JSM-5800 SEM*. This was done to analyze the fracture nature of *mPE* and the synthesized nanocomposites. For this the fracture surfaces of the samples were first coated with gold by auto sputtering.

Results and Discussion

IR Study

It is well known that *NS* is hydrophilic in nature and the surface of *NS* particles possess three types of silanol groups. These are *vicinal, geminal* and *isolated* silanol groups (Si–OH). The high bond strength of Si–O renders the surface of silica too acidic in nature and as such highly reactive towards Lewis bases. In our earlier communication,[14] the reaction between silanol groups of *NS* and oxirane group of *DGEBA* in presence of Lewis acid ($SnCl_2$) was reported.[14] Figure 1 shows the IR spectra of *NS* and *ENS*.

NS exhibits a strong IR band at 1000–1100 cm^{-1}corresponding to the Si–O–Si stretching and a broad IR band at about 3436 cm^{-1}, corresponds to the O–H stretching of surface silanol groups. The spectrum of *ENS* in comparison to the spectrum of *NS* shows new stretching vibration bands at 1178 cm^{-1}, 1234 cm^{-1} (Si–O–C), 827 cm^{-1}, 2931 cm^{-1} (1,4 - substituted benzene ring) and 1097 cm^{-1}, 1138 cm^{-1} (Si–O, Si–O–C). As expected, the epoxy resin is chemically connected to the surface of *NS* as shown in Scheme 1.[14]

Effect of Epoxy Resin Functionalization on Nanosilica to the Dispersion of Particles in the Polymer Matrix – TEM Study

Figure 2a–b displays the TEM micrographs of *mPE-NS* and *mPE-ENS*, respectively. Micrograph for *mPE-NS* (Figure 2(a)) shows the existence of chain like structures, which consist of agglomerates of silica particles dispersed in the *mPE* matrix. However, epoxy resin functionalization of *NS* prevents the agglomeration of *NS* particles and allows the dispersion of nanoparticles in the form of smaller aggregates of particles. This is reflected from the micrograph for *mPE-ENS* (Figure 2(b)).

Tensile Strength

In order to evaluate the reinforcing effect of nanoparticles in the *mPE* matrix, the various mechanical properties during extension have been measured. The *DGEBA*, which consists of highly strained three-membered oxirane groups can be easily opened by silanol groups (acidic groups) of *NS*, thereby breaking up the large agglomerates of nanoparticles into finer particles. This results in an increase in their degree of dispersion in the polymeric matrix. Functionalization of *NS* by *DGEBA* lowers the surface free energy of the particles and hence increases its wettability or interfacial adhesion with the polymer. During the pre-functionalization of *NS* with epoxy resin the surface hydroxyl groups of the silica nanoparticles act as nucleophiles to open up the three-membered oxirane groups of the epoxy resin, as is illustrated in Scheme 1.

Thus, the epoxy resin macromolecular chains bind themselves chemically to the surface of *NS*, thereby, preventing agglomeration of *NS* particles. This facilitates the

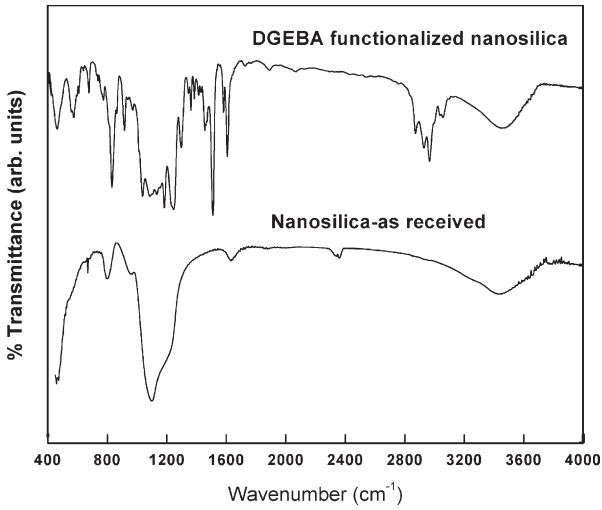

Figure 1.
IR spectra of nanosilica and epoxy resin functionalized nanosilica.

breakup of large agglomerates into smaller ones. In addition, more polar interactions (such as those due to hydrogen bonds) take place between the hydroxyl groups of epoxy resin and the surface hydroxyl groups of the silica molecules and hence improve the compatibility between the polymeric matrix and the nanoparticles. In addition, IR study also shows an enhanced compatibility between *ENS* and *mPE* because it predicts a conversion of hydrophilic surfaces into hydrophobic surfaces. The conversion of the hydrophilic surface of *NS* to a hydrophobic one may results in a better compatibility between the polymer matrix and the filler. Epoxy resin functionalization of *NS* increases the degree of dispersion of the particles as shown in Scheme 2.

Typical tensile stress-strain curves of pure *mPE* and its filled version are shown in Figure 3. It shows the reinforcing and

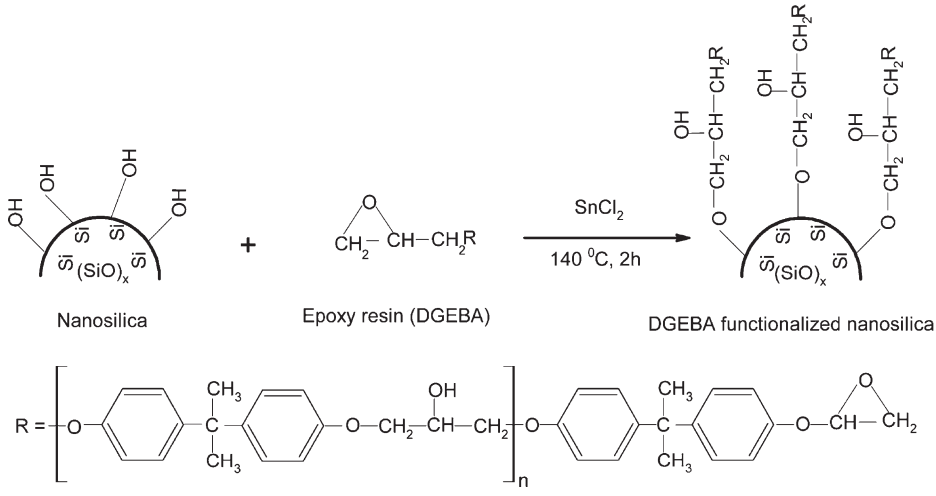

Scheme 1.
Reaction mechanism of epoxy resin functionalization on nanosilica.

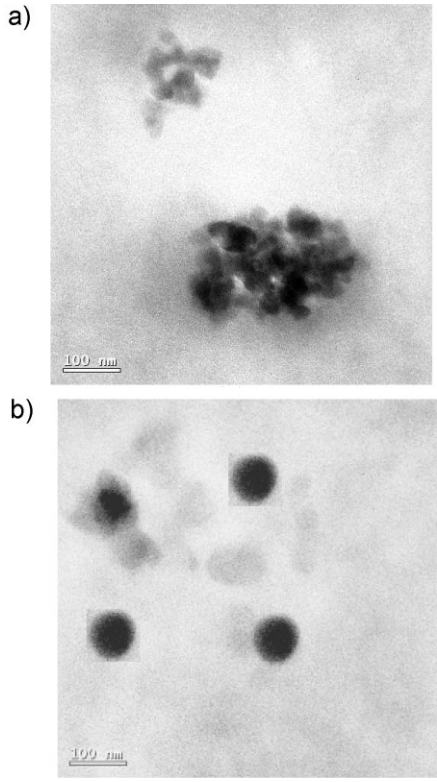

Figure 2.
TEM micrographs of mPE nanocomposites: a) nanosilca filled mPE (135000×) and, b) epoxy resin functionalized nanosilica filled PP (135000×).

toughening effects of *ENS* on the polymeric matrix. The results of tensile test have been listed in Table 2.

The stress-strain curves of pure *mPE, mPE-NS* and *mPE-ENS*, show that initially there is a steep linear increase in the tensile stress without any significant change of strain for all the samples. The yield point is

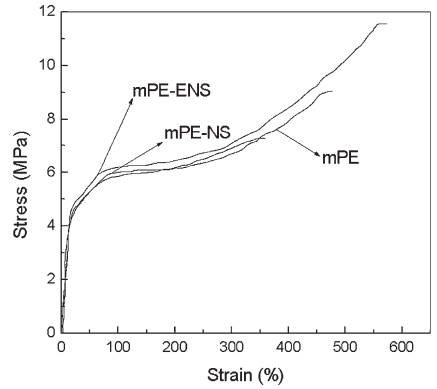

Figure 3.
Stress-strain curves of mPE nanocomposites.

attained after that. After yield point sliding of macromolecular chains takes place and they are oriented towards the direction of applied stress with proceeding strain. Lastly, the break point of the sample appears. For all the samples, the stress at break point is always fairly higher than the stress at the yield point. In case of *mPE-NS*, the yield strength is almost equivalent to pure *mPE* and ultimate tensile strength is lower. The lower ultimate tensile strength of *mPE-NS* can be attributed to the presence of agglomerated *NS* particles. These agglomerated particles contribute to a structural weakness, which may results in weak interfacial adhesion between the inorganic phase and organic phase in *mPE-NS*. However, for the *mPE-ENS*, the yield strength, ultimate tensile strength and elongation at break point are higher in comparison with *mPE-NS* and pure *mPE*. The increase in yield strength might be due to a better interface development in

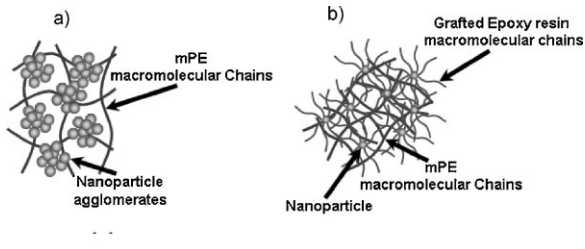

Scheme 2.
Nanoparticle dispersion in mPE matrix: a) before functionalization and, b) after functionalization.

Table 2.
Results of tensile test.

Sample configuration	Ultimate tensile strength (MPa)	Elongation at break (%)	Toughness (MJm^{-3})
mPE	9.03 ± 0.05	477 ± 5	31.29 ± 0.04
mPE-NS	7.25 ± 0.03	359 ± 7	21.69 ± 0.07
mPE-ENS	11.56 ± 0.2	573 ± 3	43.24 ± 0.05

presence of *ENS* particles between inorganic and organic phase in *mPE-ENS*. The increase in ultimate tensile strength and elongation at break point can be attributed to the presence of molecular entanglements between the epoxy resin macromolecular chains (from the surface of *NS*) and *mPE* macromolecular chains and also due to the presence of higher amount of organic phase.

In other words, in case of *mPE-ENS*, the increase in yield strength, tensile strength, toughness and elongation at break can be explained as referred in the recent work by Kontou et al.[15] Nanoparticles and polymer chains have comparable time scales for motion because of their size similarity. Due to their mobility, the nanoparticles can act as temporary crosslinks between the polymer chains, providing localized regions of enhanced strength, which in turn can retard the growth of cracks or cavities. In case of *mPE-ENS*, an efficient nanoscale dispersion of *ENS* coupled with favorable polymer-filler interactions is critical for improved toughness.

Dynamic Mechanical Analysis Results

Usually polyethylene exhibits three transitions in dynamic mechanical analysis, designated as *α-transition*, *β-transition* and *γ-transition* with decreasing temperature, which are best observed from tan δ values.[16] The *α-transition* is found to be in the wide temperature range from 0 to 120 °C, the *β-transition* occurs in the temperature range from −30 to10 °C and the *γ-transition* occurs in the temperature range from −150 to −120 °C.[16,17]

In general, the *α-transition* is attributed to the vibrational or reorientational motion of molecular chains within the crystals. The molecular mechanism involving *α-transition* is same as the one observed in the *γ-transition*.[18] It has been found that *α-transition* varies with the degree of crystallinity. In general, linear polyethylenes with high degree of crystallinity show strong *α-transition*, but in the case of polyethylene copolymers the *α-transition* tends to decrease or even disappear, with an increase in the co-monomer content.[16–18] The *α-transition* depends on the side-branch content, crystallization method and some possible mechanisms of crystallization.

Dynamic mechanical properties of the *mPE*, *mPE* filled with *NS* and *mPE* filled with *ENS* have been presented in Table 3 and the results have been compared with pure *mPE*. The variation of storage modulus, loss tangent of *mPE* and the synthesized nanocomposites against temperature are depicted in Figure 4 and 5. The glass transition temperature (T_g) of pure *mPE*, at the position of tan $\delta_{max} = 0.17$, occurs at 5 °C. It is observed that incorporation of *NS* into *mPE* does not change the tan δ_{max} value significantly (0.16 from 0.17) and hence there is no noticeable change in the glass transition temperature. However, for *mPE-NS*, *E'* (*storage modulus*) at room temperature is increased by 3%. A shift in T_g by

Table 3.
Dynamic mechanical properties of mPE nanocomposites.

Sample configuration	T_β (°C)	tan δ_{max}	E' at 25 °C (GPa)
mPE	5 ± 2	0.17 ± 0.03	1.06 ± 0.02
mPE-NS	5 ± 3	0.16 ± 0.05	1.10 ± 0.04
mPE-ENS	8 ± 1	0.15 ± 0.02	1.46 ± 0.01

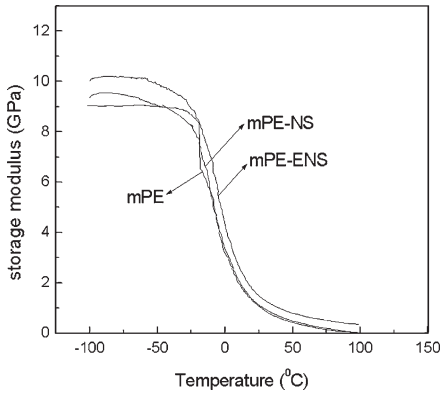

Figure 4.
Storage modulus as a function of temperature of mPE and mPE nanocomposites.

+ 5 °C, and an increase of E' at 25 °C by 37% are observed in the case of *mPE* filled with *ENS*.

The storage modulus increases with the addition of nanosilica fillers. A nanocomposite matrix can be viewed as a combination of two parts. One is nanoparticle free polymer part and another is interphase between the nanosilica and polymer. In the free part the state of the macromolecular chains is the same as that of *mPE*. Whereas, in the interphase there might be chemical or physical adsorption of *mPE* and/or transcrystallization of *mPE* on the *NS* surface. The interaction between *mPE* and *NS* becomes stronger the larger the interfacial area of *NS* particles and the greater the volume of inter-phase[15] and the interaction is mostly physical in nature. Since the macromolecular chains of interphase are restricted to the nanofiller surface the molecular motion is greatly limited. As a result the storage modulus of interphase is higher than that of the free part. The stiffness of the *NS* particles in combination with the higher interphase storage modulus, the over all storage modulus of the *mPE-NS* nanocomposites increases with the addition of *NS* particles. In addition to the physical interactions between the particle and polymer, chemical functionalization of *NS* by *DGEBA* further improves the interaction at the interphase between *ENS* and *mPE* by chemical interaction and the overall storage modulus improves further as evident in Figure 4.

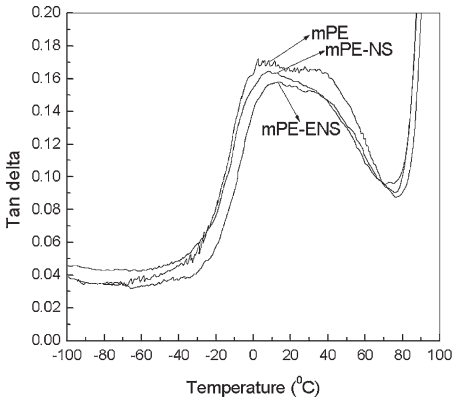

Figure 5.
Loss factor curves as a function of temperature of mPE and mPE nanocomposites.

In case of *mPE-NS*, the glass transition temperature of *mPE* remains the same and this suggests that there is not a very high interaction between nanosilica and *mPE* macromoecular chains. In case of *mPE-ENS*, the glass transition temperature of *mPE* is shifted towards a higher temperature side, suggesting a possible above-mentioned interaction between *ENS* and *mPE* macromolecular chains. Another possible explanation for the shift in glass transition temperature towards higher temperature side in case of *mPE-ENS* is due to the formation of physical entanglements between epoxy resin macromolecular chains from the surface of *NS* and *mPE* macromolecular chains.

Thermal Properties

TGA Study

An important characteristic of polymers and composites is their thermal stability at elevated temperatures. Figure 6 shows the TGA thermograms of pure *mPE* and the synthesized nanocomposites taken in an inert nitrogen atmosphere. The corresponding parameters have been given in Table 4. Thermal degradation of *mPE* in nitrogen exhibits single step degradation. Also, *mPE-NS* and *mPE-ENS* exhibits single

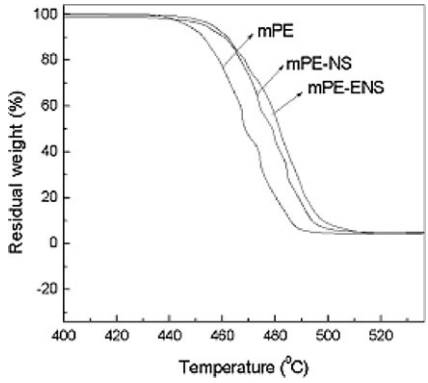

Figure 6.
TGA themograms of mPE and mPE nanocomposites.

step degradation in an inert nitrogen atmosphere. However, in presence of nanofillers the onset of thermal degradation temperature (taken at 5 wt. % loss) of *mPE* is shifted to a higher temperature side. It is observed that the onset of degradation temperature for *mPE-NS* (454 °C) is around 7 °C higher than the pure *mPE* (447 °C). In case of *mPE-ENS* the onset degradation temperature (457 °C) is increased by 10 °C with respect to pure *mPE*.

This suggests an improvement in thermal stability for *mPE-ENS*. This extent of increase in thermal stability may be due to the existence of physical entanglements between *mPE* and epoxy resin-macromolecular chains of *ENS*. This can be a reason for the reduced rate of degradation for *mPE-ENS*. These entanglements restrict the thermal motion of the *mPE* chains. In fact, the degradation temperature for *mPE-ENS* occurs relatively at a higher temperature side with respect to *mPE-NS* and pure *mPE*. This implies that *ENS* significantly enhances the thermal stability of *mPE*. Gilman[19] suggested that the high thermal stability of polymers in presence of fillers is due to the hindered thermal motion of polymer molecular chains.

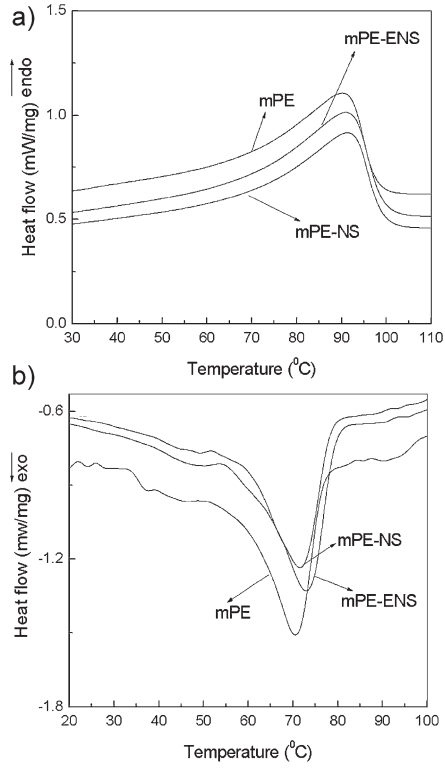

Figure 7.
DSC thermograms of mPE and mPE nanocomposites: a) second heating and, b) second cooling.

DSC Study

DSC thermograms of the pure *mPE* and synthesized nanocomposites are shown in Figure 7a–b and the corresponding parameters are given in Table 5 the degree of crystallinity of the composites has been measured using the formula given bellow.

$$x = \frac{\Delta H_m}{\Delta H_0 \times \frac{m_p}{m_c}} \times 100\%$$

Table 4.
Results of TGA study.

Sample configuration	Temp. of 5% weight loss (°C)	Temp. of 10% weight loss (°C)	Temp. of 50% weight loss (°C)
mPE	447 ± 3	452 ± 3	468 ± 4
mPE-NS	454 ± 2	459 ± 1	479 ± 3
mPE-ENS	457 ± 1	461 ± 2	482 ± 1

Table 5.
Results of DSC studies.

Sample configuration	Melting temp. (°C)	Crystallization temp. (°C)	Melting enthalpy, ΔH_c (Jg^{-1})	Crystallization enthalpy, ΔH_m (Jg^{-1})
mPE	89	70	24	42
mPE-NS	90	71	22	41
mPE-ENS	90	73	21	40

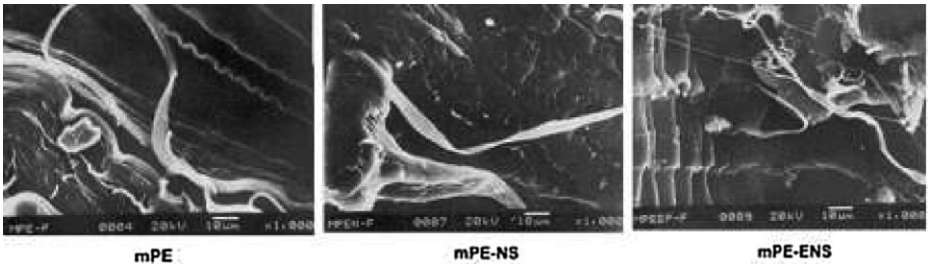

Figure 8.
SEM micrographs of tensile fracture surfaces of mPE and mPE nanocomposites.

where,

$x =$ % of crystallinity of composite.
$\Delta H_m =$ melting enthalpy (J/g) of *mPE*.
$\Delta H_0 =$ melting enthalpy (290 J/g) of 100% crystalline *PE*.[20]
$m_p =$ mass (g) of the *mPE*.
$m_c =$ mass (g) of the composite.

The melting temperature (Figure 7a) of *mPE* remains same in the presence of both kinds of nanofillers. The crystallization thermograms of pure *mPE* and the synthesized nanocomposites are shown in Figure 7(b). The *mPE* shows an exothermic crystallization peak at 70 °C. A crystallinity of 8% is calculated from the measurements obtained from melting enthalpy. The *mPE-NS* shows a crystallization peak at 71 °C with a corresponding crystallinity of 7%. In case of *mPE-ENS*, the crystallization peak is increased to 73 °C, with a corresponding crystallinity of 7%. The observed decrease in crystallinity of *mPE-NS* from the DSC measurements can be explained as follows. The adsorption of *mPE* macromolecular chains on the surface of *NS*, suggests polymer uncoiling and transformation of structures from higher energy to lower energy. But this effect is more predominant in case of *mPE-ENS* due to the formation of physical cross-links between *mPE* macromolecular chains and epoxy resin macromolecular chains (from the surface of *NS*). The shift in crystallization temperature towards higher temperature side may be due to the nucleating capability of *NS* as well as *ENS*.

Fracture Morphology

SEM Study

The SEM micrographs of the fractured surface obtained during tensile testing of the pure *mPE* and synthesized nanocomposites are shown in Figure 8.

The pure *mPE* fracture surface exhibits clear signs of plastic deformation and orientation of macromolecular chains in the direction of applied stress. A coarser appearance can be observed on the fracture surface of *mPE-NS* with little plastic deformation in the direction of applied stress. In contrast, *mPE* filled with *ENS* shows a clear evidence of plastic deformation. In addition the fracture surface of *mPE-ENS* also shows an existence of shear bands and cavities surrounded by fibrillated circles of matrix.

Conclusions

The *NS* particles were surface functionalized with *DGEBA*. The nanocomposites of mPE with *NS* and *ENS* were syntheized by conventional, econemically and industrially feasible melt blending technique. Surafce functionalization of *NS* particles with *DGEBA* has lead to improved dispersion *ENS* particle in the *mPE* matrix. This was further supported by TEM study which shows a good dispersion of *ENS* particles in case of *mPE-ENS*. Finally, SEM study suggests that *mPE-ENS* shows an extensive plastic deformation in comparison to pure *mPE* and *mPE-NS*.

[1] S. Bensason, J. Minick, A. Moet, S. Chum, A. Hiltner, E. Baer, *J Polym Sci, Part B: Polym Phys.* **1996**, *34*, 1301.
[2] S. Bensason,, S Nazarenko,, S. Chum,, A. Hiltner,, E. Baer,, *Polymer* **1997**, *38*, 3513.
[3] S. Bensason,, S. Nazarenko,, S. Chum,, A. Hiltner,, E. Baer,, *Polymer* **1997**, *38*, 3913.
[4] S. Bensason,, E.V. Stepanov,, S. Chum,, A. Hiltner,, E. Baer,, *Macromolecules* **1997**, *30*, 2436.
[5] S. Ray,, A.K. Bhowmick,, *Polymer. Eng. Sci.* **2004**, *44*, 163.
[6] R.W. Hausslein,, G.J. Fallik,, *J. Appl. Polym. Sci., Appl. Polym. Symp.* **1969**, *11*, 119.
[7] J. Gahde,, V. Muller,, Y.V. Lebedev,, Y.S. Lipatov,, *Polym. Sci. USSR* **1977**, *19*, 1446.
[8] D.H. Solomon,, M.J. Rosser,, *J Appl. Polym. Sci.* **1965**, *9*, 1261.
[9] C. Velasco-Santos,, A.L. Martinez-Hemandez,, M. Lozada-Cassou,, A. Alvarez-Castillo,, V.M. Castano,, *Nanotechnology* **2002**, *13*, 495.
[10] G. Carrot,, D. Rutot-Houze,, A. Pottier,, P. Degee,, J. Hilborn,, P. Dobois,, *Macromolecules* **2002**, *35*, 8400.
[11] O. Urzua-Sanchez,, A. Licea-Claverie,, J. Gonzalez,, L. Cota,, F. Castillon,, *Polym. Bull.* **2002**, *49*, 39.
[12] J. Lin,, J.A. Siddiqui,, R.M. Ottenbrite,, *Polym. Adv. Technology* **2001**, *12*, 285.
[13] C.S. Reddy,, C.K. Das,, *Composite Interface* **2005**, *11*, 687.
[14] C.S. Reddy,, C.K. Das,, *Polymer Composites* **2005**, *26*, 806.
[15] E. Kontou,, M. Niaounakis,, *Polymer* **2006**, *47*, 1267.
[16] N.G. Mc Crum,, B.E. Read,, G. Williams,, *Anelastic and Dielectric Effects in Polymeric Solids* Dover Publications New York **1991**.
[17] R. Popli,, M. Glotin,, L. Mandelkern,, R.S. Benson,, *J. Polym. Sci., Part B: Polym. Phys.* **1984**, *22*, 407.
[18] J. Rault,, *J. Macromol. Sci. Rev. : Macromol. Chem. Phys.* **1997**, *C37*(2), 335.
[19] J.W. Gilman,, *Appl. Clay. Sci.* **1999**, *15*, 31.
[20] J. Lu,, H.J. Sue,, T.P. Rieker,, *J. Mater. Sci.* **2000**, *35*, 5169.

